

Reaction of Dirhodium(II) Tetraacetate with *S*-Methyl-*L*-cysteine

Valerie Brunskill, Alejandra Enriquez Garcia, Farideh Jalilehvand, Benjamin S. Gelfand,
and Mengya Wu*

Department of Chemistry, University of Calgary, Calgary, AB, Canada T2N 1N4

Keywords: Dirhodium(II) acetate; *S*-methyl-*L*-cysteine; ESI-MS; UV-vis spectroscopy; Crystal structure

ABSTRACT

The reaction of antitumor active dirhodium(II) tetraacetate, $\text{Rh}_2(\text{AcO})_4$, with *S*-methyl-*L*-cysteine (HSMC) was studied at the pH of mixing (= 4.8) in aqueous media at various temperatures under aerobic conditions. The results from UV-vis spectroscopy and electrospray ionization mass spectrometry (ESI-MS) showed that HSMC initially coordinates via its sulfur atom to the axial positions of the paddlewheel framework of the dirhodium(II) complex, and was confirmed by the crystal structure of $[\text{Rh}_2(\text{AcO})_4(\text{HSMC})_2]$. After some time (48 hours at 25 °C), or at elevated temperature (40 °C), Rh-SMC chelate formation causes breakdown of the paddlewheel structure, generating the mononuclear Rh(III) complexes $[\text{Rh}(\text{SMC})_2]^+$, $[\text{Rh}(\text{AcO})(\text{SMC})_2]$ and $[\text{Rh}(\text{SMC})_3]$, as indicated by ESI-MS. These aerobic reaction products of $\text{Rh}_2(\text{AcO})_4$ with HSMC have been compared with those of the two proteinogenic sulfur-containing amino acids methionine and cysteine. The comparison shows that the (*S,N*)-chelate ring size influences the stability of the $\text{Rh}_2(\text{AcO})_4$ paddlewheel cage structure and its $\text{Rh}^{\text{II}}\text{-Rh}^{\text{II}}$ bond, when an amino acid with a thioether group coordinates to dirhodium(II) tetraacetate.

1. INTRODUCTION

The first synthesis of a dirhodium(II) carboxylate compound was reported in 1960.¹ A decade later, Bear et al. discovered their antitumor activity when treating mice bearing L1120 tumors.² Since then the properties of dirhodium(II) carboxylates, $\text{Rh}_2(\mu\text{-RCOO})_4$, have been further explored as catalysts promoting enantioselectivity and chemoselectivity (with chiral R ligands),³ as metal-organic porous materials adsorbing small molecules,⁴ and as potential antitumor agents.⁵⁻⁷ However, the mechanism of their antitumor activity is still debated.^{5, 8-12}

Dirhodium(II) tetraacetate, $\text{Rh}_2(\text{AcO})_4$ (**1**) ($\text{AcO}^- = \text{CH}_3\text{COO}^-$), has four bridging acetate ligands that form a paddlewheel cage structure around the $\text{Rh}^{\text{II}}\text{-Rh}^{\text{II}}$ bond, with two available binding sites in the axial positions (see Scheme 1). The axially coordinated ligands (L) form labile mono- or di-adducts depending on the ligand concentration, $[\text{Rh}_2(\mu\text{-RCOO})_4\text{L}_{1-2}]$,¹³ which display different colors related to the type and strength of the donor atom: generally blue or green for oxygen donor ligands, red or pink for nitrogen, and burgundy or orange for phosphorous or sulfur.¹

Thiol-containing proteins and peptides such as glutathione (γ -L-glutamyl-L-cysteinylglycine), the most abundant thiol-containing peptide in cells, can reduce the antitumor efficiency of dirhodium(II) carboxylates under aerobic conditions.¹⁴ The two sulfur-containing proteinogenic amino acids cysteine and methionine react differently with dirhodium(II) carboxylates *in vitro*. Cysteine is known to break down their paddlewheel structures, resulting in oligomeric thiolate bridged Rh(III) species,^{5, 15} while the thioether (-S-CH₃) group of methionine (HMet) initially binds reversibly to the axial positions (see Scheme 1).^{16, 17} We recently showed that the reaction of $\text{Rh}_2(\text{AcO})_4$ with methionine in aqueous media over a period of time at room

temperature, or when heated to near body temperature (40 °C) for ~3 h, proceeds to displacement of two *cis*-acetate groups and formation of a stable water-soluble $[\text{Rh}_2(\text{AcO})_2(\text{Met})_2]$ complex with tridentate binding of the Met ligands to the Rh(II) ions, both in axial and equatorial positions.¹⁸ Such reaction would also reduce the antitumor activity of the dirhodium(II) complexes, as the availability of their axial positions seems to be essential for their activity.¹⁹

The amino acid side chains in cysteine (-CH₂SH) and methionine (-CH₂CH₂-S-CH₃), Scheme 1, can form 5 and 6-membered (*S,N*)-chelate rings with metal ions, respectively.²⁰ Our previous results^{9, 10} led us to consider whether their different reactivity towards dirhodium(II) carboxylates depends not only on their functional sulfur groups (thiol *vs.* thioether) but also on the chelate ring size that they form with the rhodium ions. To test this hypothesis, we studied the reaction of *S*-methyl-*L*-cysteine with $\text{Rh}_2(\text{AcO})_4$ in aqueous media, the results of which are presented here.

S-methyl-*L*-cysteine (HSMC) is a non-proteinogenic amino acid, which can form *in vivo* by methylation of cysteine residues,²¹ and is found in some plants.²² It is naturally excreted in human urine and is a protective agent against oxidative stress.²³ HSMC has three sites for metal binding: carboxylate ($\text{pK}_{\text{a}1} = 2.14$), amine ($\text{pK}_{\text{a}2} = 9.22$) and the thioether S atom in the side chain ($I = 0.10 \text{ M}$; 25°C).²⁴ HSMC coordinates to Pd(II) and Pt(II) ions via its thioether and amino groups (*S,N*-SMC),^{25, 26} while with Co(III) and Cu(II) (*O,N*-SMC) chelates form.^{27, 28} It can bind to Rh(III) ions both in monodentate or bidentate fashion (*S,O*- or *S,N*-SMC),²⁹ and also to Ag(I) ions depending on pH (*S*-HSMC at pH < 4.5 and *S,N*-SMC at pH > 4.5).²⁴ Tridentate coordination of *S*-methyl-*L*-cysteine to half-sandwich complexes of platinum family metal ions (Ru, Os, Rh, Ir) has been observed.³⁰ Pneumatikakis et al. reported an orange-violet aqueous solution of the $[\text{Rh}_2(\text{AcO})_4(\text{S-HSMC})_2]$ adduct when mixing $\text{Rh}_2(\text{AcO})_4$ and HSMC in mole ratio

1:2. The absorption band at 558 nm of this adduct in aqueous solution was blue-shifted relative to $[\text{Rh}_2(\text{AcO})_4(\text{H}_2\text{O})_2]$ at 584 nm, indicating axially bound HSMC sulfur atoms to the dirhodium(II) core.³¹ Głaszczka et al. found that aqueous $\text{Rh}_2(\text{AcO})_4$ solutions with HSMC produced red to violet solutions for HSMC to $\text{Rh}_2(\text{AcO})_4$ mole ratios from 0.5 to 2.5. The ^1H NMR spectra of the mixtures showed a down-field shift for the SCH_3 signal relative to that of the pure ligand ($\Delta\delta_{\text{H}} = 0.22 \sim 0.25$ ppm), again indicating sulfur coordination.¹³

Here we present results on the reaction of $\text{Rh}_2(\text{AcO})_4$ with *S*-methyl-*L*-cysteine in aqueous solution at the pH of mixing (= 4.8), both at room temperature and at 40 °C (close to body temperature), using UV-vis spectroscopy and electrospray ionization mass spectrometry (ESI-MS). We compare how *S*-methyl-*L*-cysteine and methionine with the same functional groups react with $\text{Rh}_2(\text{AcO})_4$, and how their chelate ring sizes influence the nature and stability of the products.

2. EXPERIMENTAL SECTION

2.1 Materials

Dirhodium(II) tetraacetate and *S*-methyl-*L*-cysteine were purchased from Pressure Chemical Company and Sigma-Aldrich, respectively; both were used without further purification. The Sephadex G-15 used as stationary phase in the size-exclusions column chromatography was purchased from GE Healthcare Life Sciences. pH measurements were made using a calibrated VWR Symphony SB70P pH meter.

2.2 Sample Preparation

Titration of $\text{Rh}_2(\text{AcO})_4$ with *S*-methyl-*L*-cysteine. A 2.00 mM emerald green stock solution of $\text{Rh}_2(\text{AcO})_4$ (0.0500 mmol in 25.00 mL) and a 0.200 M stock solution of HSMC (1.000 mmol in

5.00 mL) were prepared in distilled water. The UV-vis absorption spectrum of 0.30 mL $\text{Rh}_2(\text{AcO})_4$ solution (0.60 μmol) was measured in a quartz cuvette with 1 mm path length. After adding 3.00 μL (0.60 μmol) of the HSMC stock solution, the cuvette was shaken and the UV-vis absorption spectrum collected again. This process was repeated by subsequent additions of 3.00 μL aliquots of the stock HSMC solution to the cuvette, measuring the UV-vis spectra of solutions containing $\text{Rh}_2(\text{AcO})_4$: HSMC mole ratios 1:1 to 1:40, in which C_{Rh_2} changed from 1.98 to 1.43 mM.

Preparation of $[\text{Rh}_2(\text{AcO})_4(\text{HSMC})_2]$ (3). A solution of S-methyl-L-cysteine (0.226 mmol) in 2.5 mL of water was added to an emerald green suspension of $\text{Rh}_2(\text{AcO})_4$ (0.1123 mmol) in 10 mL of water. The resulting violet solution was stirred for 5 minutes and filtered through a 0.45 μm polyethersulfone (PES) syringe filter to remove any potential unreacted dirhodium(II) tetraacetate. The filtered mixture was evaporated to ~ 1 mL. Purple crystals were obtained using acetone in a vapour diffusion setup overnight at room temperature. For elemental analysis, the crystals were filtered and dried in a desiccator under vacuum. Elemental anal. calcd for $[\text{Rh}_2(\text{AcO})_4(\text{HSMC})_2]$ ($\text{Rh}_2\text{C}_{16}\text{H}_{30}\text{N}_2\text{O}_{12}\text{S}_2$): %C 26.98, %H 4.24, %N 3.93; Found %C 27.04, %H 4.58, %N 3.77. IR (cm^{-1}): 1578, 1407, 1344, 1046, 960, 693 (Figure S1).

Solution of $\text{Rh}_2(\text{AcO})_4$ with excess S-methyl-L-cysteine studied at various temperatures. To an aqueous solution of $\text{Rh}_2(\text{AcO})_4$ (0.0602 mmol in 25.00 mL), 5.00 mL of a 0.479 M aqueous solution of HSMC was added, resulting in a violet-purple solution ($C_{\text{Rh}_2} = 2.01$ mM, $C_{\text{HSMC}} = 79.8$ mM, pH = 4.81). The reaction mixture was monitored for 35 days at room temperature, using UV-vis absorption spectroscopy, and electrospray ionization mass spectrometry (ESI-MS).

A similar solution was prepared maintaining the reaction temperature at 40 °C, and was monitored by UV-vis and ESI-MS for 15 days, until no further changes occurred. Another solution with similar composition was refluxed for an hour at 100 °C before measuring its UV-vis absorption and ESI-mass spectra.

2.3 Physical Measurements and Methods

Electronic Spectroscopy. The UV-vis absorption spectra were obtained at room temperature by means of a Cary 300 UV-vis double-beam spectrophotometer, using a pair of 1 mm path-length quartz cuvettes, with distilled water as reference.

Electrospray Ionization Mass Spectrometry (ESI-MS). The ESI-mass spectra were measured with an Agilent 6520 Q-ToF mass spectrometer, both in + and – ion modes. The samples, further diluted with methanol, were injected and mobilized with a flow rate of 0.2 mL/min rate and a drying gas flow rate at 7 L/min at 200 °C. The fragmentor, capillary and skimmer voltages were set to 80 V, 4000 V and 65 V, respectively. The peaks in the mass spectra were identified using an isotope distribution calculator from Scientific Instrumentation Services, Inc. (SIS).³²

Vibrational spectroscopy. IR spectra were measured using an Agilent Cary 630 FT-IR with a diamond ATR accessory.

Single crystal X-ray diffraction. Purple crystals of $[\text{Rh}_2(\text{AcO})_4(\text{HSMC})_2] \cdot 3\text{H}_2\text{O}$ (**3** + 3H₂O) were grown by vapour diffusion of acetone into a saturated aqueous solution of **3**. A single crystal was mounted on a glass loop using Paratone. Diffraction data were collected at 100 K on a Nonius Kappa diffractometer (Mo K_α radiation, $\lambda = 0.71069 \text{ \AA}$) equipped with an AEX-II CCD detector. Diffractions spots were integrated and scaled with SAINT,³³ and minor twinning components were resolved and removed with TWINABS, as only one component diffracted strongly. The

space group was determined with XPREP.³⁴ Using Olex2,³⁵ the structure was solved with the ShelXS using Direct Methods, followed by refinements with ShelXL.³⁶ H atoms of water molecules were placed in calculated H-bonding positions; other H atoms were placed in geometrically calculated positions. Electron density contributions from diffuse solvent molecules were modeled using the SQUEEZE routine in PLATON.³⁷

3 RESULTS AND DISCUSSION

3.1 Formation of Rh₂(AcO)₄ adducts with *S*-methyl-*L*-cysteine

Figure 1 (*left*) displays the UV-vis absorption spectra of a 2.00 mM aqueous solution of Rh₂(AcO)₄ (**1**), and its mixtures with increasing amounts of *S*-methyl-*L*-cysteine to obtain solutions with Rh₂(AcO)₄ : HSMC mole ratios from 1:1 to 1:40. The color change from emerald green to violet-purple is associated with a blue-shift of λ_{\max} in the visible region from 584 nm to 543 nm (see the inset). This peak, which is attributed to the $\pi^*(\text{Rh}_2^{4+}) \rightarrow \sigma^*(\text{Rh}_2^{4+})$ transition of the Rh^{II}-Rh^{II} bond, is sensitive to the nature of the donor atom in the axial position of **1**.^{1, 38} Its gradual shift occurs as sulfur atoms from HSMC molecules increasingly replace the axially bound water molecules in [Rh₂(AcO)₄(H₂O)₂]. The intense peaks simultaneously appearing in the UV-region at 279 and 304 nm are related to the $\sigma(\text{Rh}_2^{4+}) \rightarrow \sigma^*(\text{Rh}_2^{4+})$ transition in the mono- and di-adducts, [Rh₂(AcO)₄(HSMC)(H₂O)] (**2**) and [Rh₂(AcO)₄(HSMC)₂] (**3**), respectively. Similar absorption bands were observed for the Rh₂(AcO)₄-methionine adducts: [Rh₂(AcO)₄(HMet)(H₂O)] (283 nm), and [Rh₂(AcO)₄(HMet)₂] (307 nm and 540 nm).¹⁸

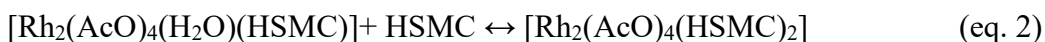
The UV-vis absorption spectrum of the aqueous Rh₂(AcO)₄ : HSMC solution with mole ratio 1:40 ($C_{\text{Rh}_2} = 1.43$ mM) shows a large absorption band at $\lambda_{\max} = 304$ nm, indicating that the di-adduct [Rh₂(AcO)₄(HSMC)₂] (**3**) dominates. However, the ESI-mass spectrum of this solution in (+) ion mode showed only a mass peak for [Rh₂(AcO)₄(HSMC) + H⁺] ($+m/z = 577.91$ amu),

and no peak for **3**; see Figure 1 (*right*). This is probably due to the dilution with MeOH before injection, leading to replacement of one of the HSMC ligands in **3** with a solvent molecule.

The relative amounts of $[\text{Rh}_2(\text{AcO})_4(\text{H}_2\text{O})_2]$, and the *S*-methyl-*L*-cysteine adducts **2** and **3** were tentatively determined by performing the peak-fitting procedure on peaks at 279 and 304 nm, using the Origin Pro program (see Supplemental Online Materials Figure S2 and Table S1). The mean stability constants could then be estimated for the 1:1 and 1:2 adducts (see Table S2):



$$K_1 = 3.85 \times 10^{-2} \pm 3.8 \times 10^{-3}$$



$$K_2 = 8.94 \times 10^{-2} \pm 8.5 \times 10^{-3}$$

These formation constants of the mono- and di-adducts **2** and **3** are much lower than those for $\text{Rh}_2(\text{AcO})_4$ adducts with imidazole ($K_1 = 6826 \pm 265$; $K_2 = 171 \pm 15$),³⁹ or adenosine mono-, di- and tri-phosphates ($1152 \pm 50 \leq K_1 \leq 1893 \pm 99$; $110 \pm 14 \leq K_2 \leq 202 \pm 14$).⁴⁰ This indicates that *S*-methyl-*L*-cysteine has a lower affinity for binding to the axial positions of $\text{Rh}_2(\text{AcO})_4$ compared with the above biologically relevant ligands.

Single crystal X-ray diffraction. Figure 2 displays the crystal structure of the di-adduct $[\text{Rh}_2(\text{AcO})_4(\text{HSMC})_2] \cdot 3\text{H}_2\text{O}$ (**3** + $3\text{H}_2\text{O}$), where two *S*-methyl-*L*-cysteine ligands are coordinated axially to the paddlewheel structure of $\text{Rh}_2(\text{AcO})_4$ (**1**) via their thioether group. The crystal data and structural refinement, as well as selected bond distances and bond angles are presented in Tables S3 and S4. The Rh-S bond length (2.474 – 2.484 Å) is the shortest Rh-S distance reported for a thioether axially coordinated to $\text{Rh}_2(\text{AcO})_4$ (generally ranging from 2.517 to 2.560 Å).⁴¹⁻⁴⁴

This distance is also 0.1 Å shorter than the refined distance of 2.58 ± 0.02 Å obtained for a $\text{Rh}_2(\text{AcO})_4$ methionine solution ($C_1 = 6.45$ mM, 1:2 mole ratio) by X-ray absorption spectroscopy.¹⁸ The Rh-Rh distance of 2.404(2) Å is slightly elongated relative to that of the di-aqua adduct, $[\text{Rh}_2(\text{AcO})_4(\text{H}_2\text{O})_2]$ (2.3855(5) Å),⁴⁵ but within the range for dirhodium(II) tetraacetate complexes axially coordinated to thioether ligands (2.403 – 2.413 Å).⁴¹⁻⁴⁴

3.2 Reaction of $\text{Rh}_2(\text{AcO})_4$ with excess *S*-methyl-*L*-cysteine at various temperatures

Room temperature. The reaction of $\text{Rh}_2(\text{AcO})_4$ (**1**) with excess *S*-methyl-*L*-cysteine ($C_{\text{Rh}_2} = 2.01$ mM, $C_{\text{HSMC}} = 79.8$ mM; pH = 4.81) at room temperature was monitored over a period of 28 days using UV-vis spectroscopy and ESI-MS. The violet-purple solution turned orange-red after 13 days, and then became yellow after 28 days. The UV-vis spectra are shown in Figure 3 (*left*), and the ESI-mass spectrum of the solution measured 21 days after mixing is displayed in Figure 3 (*right*). The ESI-mass spectra measured at different time intervals are presented in the Supplemental Online Material, Figures S3 and S4, with the mass peak assignments in Table S5.

Figure 3 (*left*) shows that the two absorption bands at 304 nm and 543 nm, associated with electronic transitions involving $\text{Rh}^{\text{II}} - \text{Rh}^{\text{II}}$ molecular orbitals in the $[\text{Rh}_2(\text{AcO})_4(\text{HSMC})_2]$ (**3**) adduct (see above), gradually lose intensity over time. A decreasing concentration of **3** is also consistent with the mass peaks associated with the mononuclear Rh(III) species $[\text{Rh}(\text{SMC})_2]^+$, $[\text{Rh}(\text{SMC})_2(\text{AcO})]$ and $[\text{Rh}(\text{SMC})_3]$ appearing in the ESI-mass spectra ($+m/z = 370.96$, 430.98 and 506.00 amu, respectively), in addition to those related to the dirhodium(II) adducts $[\text{Rh}_2(\text{AcO})_4(\text{HSMC})_2]$ ($-m/z = 710.93$), $[\text{Rh}_2(\text{AcO})_4(\text{HSMC})]$ ($+m/z = 577.91$) and $[\text{Rh}_2(\text{AcO})_3(\text{HSMC})]^+$ ($+m/z = 652.92$); see Table S5. The first Rh(III) mass ion was detected after 48 hours ($+m/z = 430.98$); see Figure S3.

Rhodium oxidation ($\text{Rh}_2^{\text{II}} \rightarrow 2\text{Rh}^{\text{III}} + 2e^-$) probably occurs through reduction of oxygen to peroxide ($\text{O}_2 + 2e^- \rightarrow \text{O}_2^{2-}$), as previously observed for the aerobic reaction of $\text{Rh}_2(\text{AcO})_4$ with cysteine and penicillamine.¹⁵ Mass peaks detected at $+m/z = 150.02$ and $-m/z = 152.04$ amu reveal the presence of *S*-methyl-*L*-cysteine sulfoxide (HSMC + O), which could be due to peroxide formation in solution.

The behavior of *S*-methyl-*L*-cysteine towards $\text{Rh}_2(\text{AcO})_4$ over time differs from that of methionine. Although also mononuclear Rh(III) species were detected by ESI-MS a week after mixing $\text{Rh}_2(\text{AcO})_4$ and methionine at room temperature, the purple color of the solution mixture never changed. Size-exclusion chromatography showed that dirhodium(II) species including $[\text{Rh}_2(\text{AcO})_2(\text{Met})_2]$, were still dominating even 4 weeks after initial mixing.¹⁸

Near body temperature. Keeping the reaction temperature at 40 °C for a similar $\text{Rh}_2(\text{AcO})_4$ solution ($C_{\text{Rh}_2} = 2.01$ mM) with HSMC in excess changed its color to light purple after 48 hours, then to yellow/orange after 4 days, and bright yellow after 10 days. The mixture was monitored by UV-vis and ESI-MS for 15 days (Figure 4). The breakdown of the $\text{Rh}^{\text{II}}\text{-Rh}^{\text{II}}$ bond was much faster at 40 °C than at room temperature (see Figure 3), as shown by the rapid loss of peak intensity at 543 nm and 304 nm. Mass peaks in the ESI-mass spectra related to the 1:1 $[\text{Rh}_2(\text{AcO})_4(\text{HSMC})]$ adduct ($-m/z = 575.89$; $+m/z = 577.91$ amu) could only be detected one hour after mixing. Mass peaks for the mononuclear Rh(III) species $[\text{Rh}(\text{SMC})_2]^+$ and $[\text{Rh}(\text{SMC})_2(\text{AcO})]$ ($+m/z = 307.96, 430.98$) appeared in the purple solution after 24 hours, and that of $[\text{Rh}(\text{SMC})_3]$ ($+m/z = 505.99$) was detected in the yellow/orange solution after 4 days; see Figure S5. For the bright yellow solution obtained after 10 days, only mass peaks related to Rh(III) mononuclear complexes could be detected, and the absorption peaks in the UV (290 – 320 nm) and visible (480 – 650 nm) regions had disappeared. No further changes occurred

between days 10 and 15, indicating that the reaction had reached completion. In contrast to methionine, no mass peak for an intermediate $[\text{Rh}_2(\text{AcO})_2(\text{SMC})_2]$ complex was detected during this period of 15 days.¹⁸

Reflux. When refluxing a $\text{Rh}_2(\text{AcO})_4$ – HSMC solution with similar composition at 100 °C, the initially violet mixture turned yellow after merely 45 minutes. The UV-vis absorption and ESI-mass spectra (+ and – ion modes) of the solution were measured after refluxing for an hour (see Figures S6 and S7). The absorption spectrum of this yellow solution did not show any peak in the UV (290 – 320 nm) or visible (480 – 650 nm) regions, and its ESI-mass spectra only displayed peaks corresponding to mononuclear Rh(III) complexes: $[\text{Rh}(\text{SMC})_2]^+$, $[\text{Rh}(\text{AcO})(\text{SMC})_2]$, $[\text{Rh}(\text{SMC})_3]$ and $[\text{Rh}(\text{SMC})_4]^-$. This reaction again differs from that with methionine, which generated $[\text{Rh}_2(\text{AcO})_2(\text{Met})_2]$ as a major product (~ 35%) under similar experimental conditions.¹⁸ In order to isolate pure monomeric Rh(III) species, this solution was concentrated and passed through a Sephadex G-15 size-exclusion chromatography column; different parts of the yellow band were analyzed by ESI-MS, which showed a mixture of Rh(III)-SMC complexes (Figure S8), and could not be further purified. Nor did the reaction of RhCl_3 with *S*-methyl-*DL*-cysteine yield any crystalline compound, as it did with methionine $[\text{Rh}(\text{D-Met})(\text{L-Met})]\text{Cl}$.¹⁸

4 CONCLUSION

The present study shows that $\text{Rh}_2(\text{AcO})_4$ can form an axially *S*-coordinated di-adduct $[\text{Rh}_2(\text{AcO})_4(\text{HSMC})_2]$ with *S*-methyl-*L*-cysteine (HSMC), as confirmed by X-ray crystallography. Reaction of $\text{Rh}_2(\text{AcO})_4$ with excess HSMC in aqueous solution initially forms $[\text{Rh}_2(\text{AcO})_4(\text{HSMC})_2]$ ($\lambda_{\text{max}} = 304, 543 \text{ nm}$) at room temperature (RT), similar to its reaction with methionine. Over time (~2 weeks) and under aerobic conditions at RT mononuclear Rh(III)-

SMC complexes gradually become dominating which change the solution color from purple to red/orange/yellow. The reaction proceeds faster at 40 °C (~ 4 days), and rather rapidly (~45 min) when refluxed at 100 °C, as shown by the concurrent reduction of the UV-vis peak intensities at 304 and 543 nm. The mass ions detected by ESI-MS were associated with the mononuclear Rh(III) species $[\text{Rh}(\text{SMC})_2]^+$, $[\text{Rh}(\text{AcO})(\text{SMC})_2]$, $[\text{Rh}(\text{SMC})_3]$ and $[\text{Rh}(\text{SMC})_4]^-$. However, no mass peak for a possible intermediate dimeric $[\text{Rh}_2(\text{AcO})_2(\text{SMC})_2]$ complex was observed in the solution at RT, 40 °C, or after reflux at 100 °C, in contrast to the corresponding reaction with methionine. As shown in Scheme 2, methionine (HMet) can form not only axial mono- and di-adducts $[\text{Rh}_2(\text{AcO})_4(\text{HMet})_{1-2}]$, but also a stable dirhodium(II) complex, $[\text{Rh}_2(\text{AcO})_2(\text{Met})_2]$ (~20-35% depending on temperature), as well as minor amounts of mononuclear Rh(III) methionine complexes.¹⁸

This difference in reactivity of $\text{Rh}_2(\text{AcO})_4$ with *S*-methyl-*L*-cysteine, with the same functional groups as methionine (Scheme 1), is probably an effect of the different sizes of the (*S,N*)-chelate ring that these two amino acids form with metal ions.²⁰ The 6-membered (*S,N*)-chelate ring of methionine can be further stabilized by coordination of the carboxylate oxygen atom of the tridentate Met ligand, leading to the stable dimeric $[\text{Rh}_2(\text{AcO})_2(\text{Met})_2]$ complex with fused (5+6)-membered chelates. The 5-membered (*S,N*)-chelate ring that *S*-methyl-*L*-cysteine could form in a corresponding intermediate $[\text{Rh}_2(\text{AcO})_2(\text{SMC})_2]$ would be more strained, and result in less stable (5+5)-membered joined chelate rings. While oxidation of Rh ions is promoted by formation of stable mononuclear Rh(III) complexes, probably including tridentate SMC chelates in $[\text{Rh}(\text{SMC})_2]^+$, as observed for $[\text{Rh}(\text{S,N,O-Met})_2]^+$.¹⁸

Another aspect is given by comparing the reactions with cysteine that like HSMC is able to form 5-membered (*S,N*)-chelate rings with metal ions. Cysteine with thiol as its sulfur

functional group reacts rapidly with $\text{Rh}_2(\text{AcO})_4$ under aerobic conditions to form oligomeric Rh(III) thiolate bridged complexes (Scheme 2); no monomeric Rh(III)-cysteine species were detected by ESI-MS.¹⁵

Therefore, we can conclude that the reactions of $\text{Rh}_2(\text{AcO})_4$ with sulfur-containing amino acids depend strongly on the nature of their functional sulfur group (-SH vs. -SCH₃), but also on the ring size when forming an (*S,N*)-chelate. In addition to adduct formation, thioether-containing amino acids such as *S*-methyl-*L*-cysteine and methionine can replace acetate ligands in $\text{Rh}_2(\text{AcO})_4$. Thus, already at near body temperatures also *S*-methyl-*L*-cysteine may degrade the $\text{Rh}_2(\text{AcO})_4$ cage structure and reduce its cytotoxicity *in vivo*, by promoting oxidation processes via formation of stable mononuclear Rh(III) complexes.

ASSOCIATE CONTENT

Supplemental Online Material

The Supplemental Online Material is available free of charge on the Taylor & Francis Publications website, and includes: crystal data and structure refinement of complex (**3** + 3H₂O), selected bond lengths and angles of (**3** + 3H₂O); FT-IR spectra of **1**, *S*-methyl-*L*-cysteine and complex **3**; UV peak fitting and calculation of stability constants for 1:1 and 1:2 adducts (**2** and **3**); ESI-MS time study data (+ and – ion modes) for the reaction at room temperature, 40 °C and 100 °C, as well as the UV-vis spectrum of the reaction after an hour of reflux at 100 °C.

AUTHOR INFORMATION

Corresponding Author

* E-mail: faridehj@ucalgary.ca

Disclosure Statement

The authors declare no competing financial interest.

ACKNOWLEDGEMENTS

We express our appreciation to Mr. Wade White at the instrumentation facility at the Department of Chemistry, University of Calgary, for his assistance with the ESI-MS measurements. V.J.B acknowledges the NSERC Undergraduate Student Research Awards (USRA). A.E.G appreciates the University of Calgary Eyes High, Faculty of Graduate Studies and Faculty of Science Dean's Doctoral Scholarships. M.W. visit from the China University of Petroleum to the University of Calgary was supported through China Scholarship Council. This work was financially supported by the Natural Sciences and Engineering Research Council of Canada (NSERC) funding reference number RGPIN 2016-04546, Canadian Foundation for Innovation (CFI) and the Province of Alberta (Department of Innovation and Science).

REFERENCES

1. Boyar, E. B. & Robinson, S. D. *Coord. Chem. Rev.* **50**, 109-208 (1983).
2. Hughes, R. G., Bear, J. L. & Kimball, A. P. *Proc. Am. Assoc. Cancer Res.* **13**, 120 (1972).
3. Hansen, J. & Davies, H. M. L. *Coord. Chem. Rev.* **252**, 545-555 (2008).
4. Takamizawa, S., Nataka, E.-i., Akatsuka, T., Miyake, R., Kakizaki, Y., Takeuchi, H., Maruta, G. & Takeda, S. *J. Am. Chem. Soc.* **132**, 3783-3792 (2010).
5. Howard, R. A., Spring, T. G. & Bear, J. L. *Cancer Res.* **36**, 4402-4405 (1976).
6. Katsaros, N. & Anagnostopoulou, A. *Critical Reviews in Oncology/Hematology* **42**, 297-308 (2002).
7. Chifotides, H. T. & Dunbar, K. R. Rhodium Compounds, *Multiple Bonds Between Metal Atoms*, edited by F. A. Cotton, C. A. Murillo & R. A. Walton, New York: Springer Science and Business Media Inc. (2005).
8. Bear, J. L., Gray, H. B., Jr., Rainen, L., Chang, I. M., Howard, R., Serio, G. & Kimball, A. P. *Cancer Chemother Rep* **59**, 611-620 (1975).
9. Sorasaene, K., Fu, P. K. L., Angeles-Boza, A. M., Dunbar, K. R. & Turro, C. *Inorg. Chem.* **42**, 1267-1271 (2003).
10. Dunham, S. U., Chifotides, H. T., Mikulski, S., Burr, A. E. & Dunbar, K. R. *Biochemistry* **44**, 996-1003 (2005).
11. Chifotides, H. T. & Dunbar, K. R. *Acc. Chem. Res.* **38**, 146-156 (2005).
12. Siu, F.-M., Lin, I. W.-S., Yan, K., Lok, C.-N., Low, K.-H., Leung, T. Y.-C., Lam, T.-L. & Che, C.-M. *Chem. Sci.* **3**, 1785-1793 (2012).
13. Głaszczka, R. & Jaźwiński, J. *Coord. Chem.* **69**, 3703-3714 (2016).
14. Enriquez Garcia, A., Jalilehvand, F. & Niksirat, P. *J. Biol. Inorg. Chem.* **23**, 231-239 (2018).
15. Jalilehvand, F., Enriquez Garcia, A. & Niksirat, P. *ACS Omega* **2**, 6174-6186 (2017).
16. Jakimowicz, P., Ostropolska, L. & Pruchnik, F. *Met. Based Drugs* **7**, 201-209 (2000).
17. Głaszczka, R., Jaźwiński, J., Kamiński, B. & Kamińska, M. *Tetrahedron asym.* **21**, 2346-2355 (2010).
18. Enriquez Garcia, A., Jalilehvand, F., Niksirat, P. & Gelfand, B. S. *Inorg. Chem.* **57**, 12787-12799 (2018).
19. Aguirre, J. D., Lutterman, D. A., Angeles-Boza, A. M., Dunbar, K. R. & Turro, C. *Inorg. Chem.* **46**, 7494-7502 (2007).
20. Berthon, G. *Pure & Appl. Chem.* **67**, 1117-1240 (1995).
21. Barnsley, E. A. *Biochim. Biophys. Acta* **90**, 24-36 (1963).
22. Nomura, J., Nishizuka, Y. & Hayaishi, O. *J. Biol. Chem.* **238**, 1441-1446 (1963).
23. Rubino, F. M., Pitton, M., Fabio, D. D., Meroni, G., Santaniello, E., Caneva, E., Pappini, M. & Colombi, A. *Biomedical Chromatography* **25**, 330-343 (2011).
24. Pettit, L. D., Siddiqui, K. F., Kozlowski, H. & Kowalik, T. *Inorg. Chim. Acta* **55**, 87-91 (1981).
25. Jezowska-Trzebiatowska, B., Allain, A. & Kozlowski, H. *Inorg. Nucl. Chem. Lett.* **15**, 279-284 (1979).
26. Pannala, V. A. & Raju, R. M. *Proc. Natl. Acad. Sci., India, Sect. A* **77**, 293-299 (2007).
27. Jun, M. J., Park, Y. B. & Choi, S. R. *Polyhedron* **8**, 1205-1211 (1989).
28. Patra, A. K., Nethaji, M. & Chakravarty, A. R. *J. Inorg. Biochem.* **101**, 233-244 (2007).

29. Bukanova, A. E., Sidorova, T. P. & Shubochkin, L. K. *Koordinatsionnaya Khimiya* **18**, 329-332 (1992).
30. Patalenszki, J., Bíró, L., Bényei, A. C., Muchova, T. R., Kasparikova, J. & Buglyó, P. *RSC Advances* **5**, 8094-8107 (2015).
31. Pneumatikakis, G. & Psaroulis, P. *Inorg. Chim. Acta* **46**, 97-100 (1980).
32. Manura, J. J. & Manura, D. J. *Scientific Instrument Services (SIS): Isotope Distribution Calculator and Mass Spec Plotter*, <http://www.sisweb.com/mstools/isotope.htm> (2016).
33. *SAINT*. (2017).
34. *XPREP*. (2017).
35. Dolomanov, O. V., Bourhis, L. J., Gildea, R. J., Howard, J. A. K. & Puschmann, H. J. *Appl. Cryst.* **42**, 339-341 (2009).
36. Sheldrick, G. M. *Acta Cryst. C* **71**, 3-8 (2015).
37. Spek, A. L. *Acta Cryst. C* **71**, 9-18 (2015).
38. Norman, J. G. & Kolari, H. J. *J. Am. Chem. Soc.* **100**, 791-799 (1978).
39. Das, K. & Bear, J. L. *Inorg. Chem.* **15**, 2093-2095 (1976).
40. Rainen, L., Howard, R. A., Kimball, A. P. & Bear, J. L. *Inorg. Chem.* **14**, 2752-2754 (1975).
41. Clark, R. J. H., Hempleman, A. J., Dawes, H. M., Hursthouse, M. B. & Flint, C. D. *J. Chem. Soc. Dalton Trans.* 1775-1780 (1985).
42. Basato, M., Biffis, A., Martinati, G., Zecca, M., Ganis, P., Benetollo, F., Aronica, L. A. & Caporusso, A. M. *Organometallics* **23**, 1947-1952 (2004).
43. Matsubayashi, G.-e., Yokoyama, K. & Tanaka, T. *J. Chem. Soc. Dalton Trans.* 3059-3062 (1988).
44. Cotton, F. A. & Felthouse, T. R. *Inorg. Chem.* **19**, 323-328 (1980).
45. Cotton, F. A., DeBoer, B. G., LaPrade, M. D., Pipal, J. R. & Ucko, D. A. *Acta Cryst. B* **27**, 1664-1671 (1971).

Scheme 1

Figure 1. *Left*) UV-vis absorption spectra of aqueous solutions of $\text{Rh}_2(\text{OAc})_4$ ($C_{\text{Rh}_2} = 2.00$ mM), and its mixtures with *S*-methyl-*L*-cysteine in increasing mole ratios (from 1:1 to 1:40 for $C_{\text{Rh}_2} = 1.98$ to 1.43 mM); the molar absorption coefficients have been corrected for the changes in C_{Rh_2} . *Right*) ESI-Mass spectrum (+ ion mode) of the solution containing $\text{Rh}_2(\text{OAc})_4$ and HSMC in mole ratio 1:40; $C_{\text{Rh}_2} = 1.43$ mM, with 100% intensity assigned to the mass peak at $+m/z = 136.04$ amu (atomic mass unit) for $[\text{HSMC} + \text{H}^+]^+$ ion.

Figure 2. Crystal structure of $[\text{Rh}_2(\text{AcO})_4(\text{L-HSMC})_2] \cdot 3\text{H}_2\text{O}$ (**3** + $3\text{H}_2\text{O}$); H atoms and water molecules are omitted for clarity.

Figure 3. (*Left*) UV-vis absorption spectra of an aqueous $\text{Rh}_2(\text{AcO})_4$ solution with *S*-methyl-*L*-cysteine in excess ($C_{\text{Rh}_2} = 2.01$ mM, $C_{\text{HSMC}} = 79.8$ mM; pH = 4.81; 25 °C) during 28 days; (*right*) ESI-mass spectrum (+ ion mode) of the solution measured Day 21 after mixing at room temperature, with 100% intensity for the mass peak at $+m/z = 136.04$ amu for $[\text{HSMC} + \text{H}^+]^+$ ion.

Figure 4. (*Left*) UV-vis absorption spectra of an aqueous solution of $\text{Rh}_2(\text{AcO})_4$ and excess *S*-methyl-*L*-cysteine ($C_{\text{Rh}_2} = 2.01$ mM, $C_{\text{HSMC}} = 79.8$ mM; pH = 4.81; 40 °C) measured over a period of 10 days after mixing.

Scheme 2. Aerobic reaction products of $\text{Rh}_2(\text{AcO})_4$ with the sulfur-containing amino acids: cysteine, methionine and *S*-methyl-*L*-cysteine.

Scheme 1

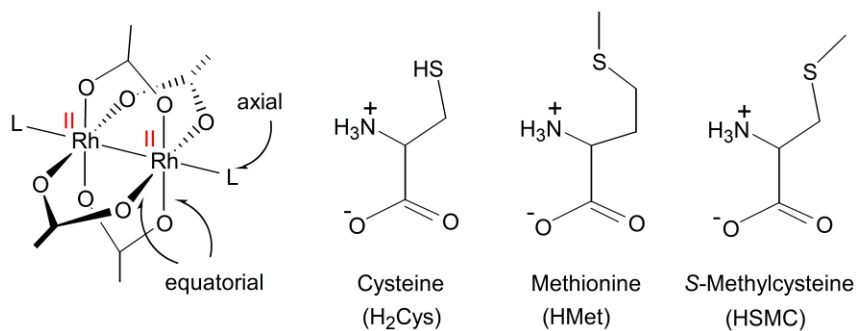


Figure 1 (Left)

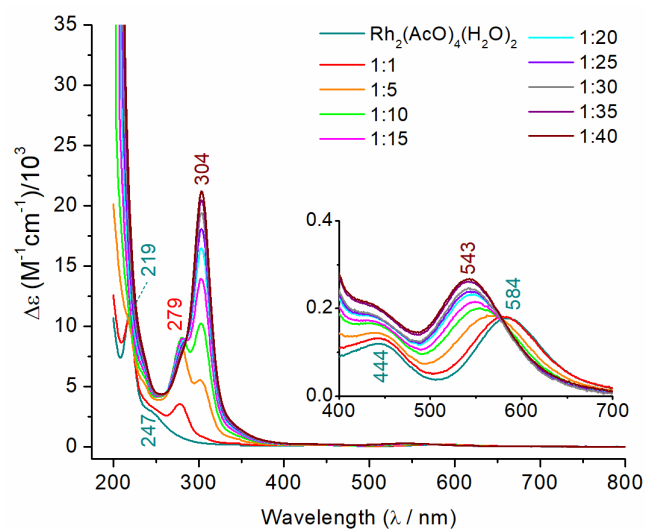


Figure 1 (Right)

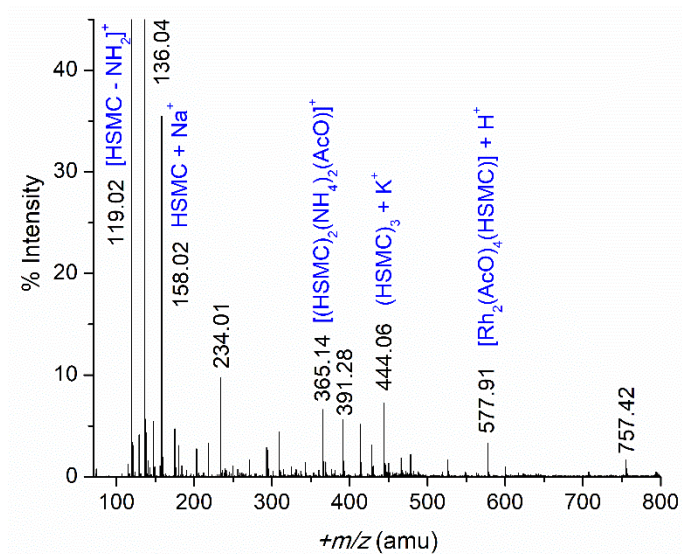


Figure 2

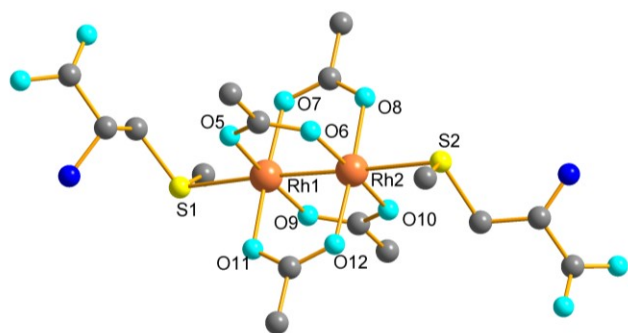


Figure 3 (Left)

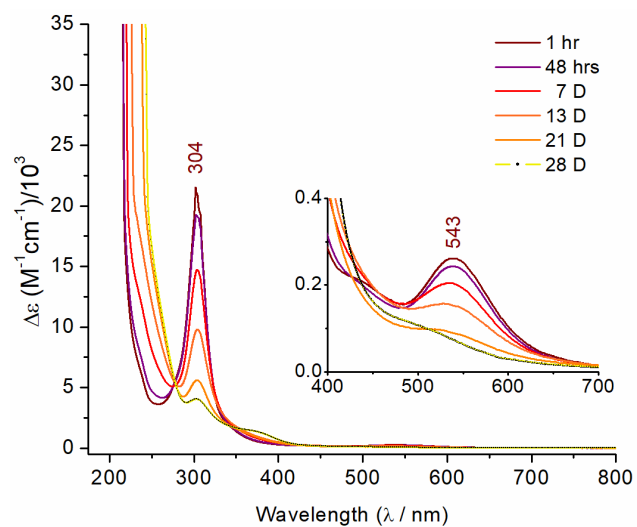


Figure 3 (Right)

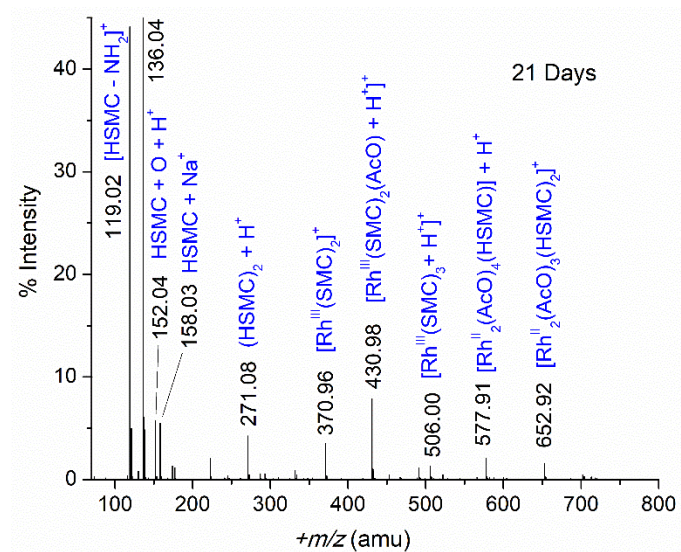
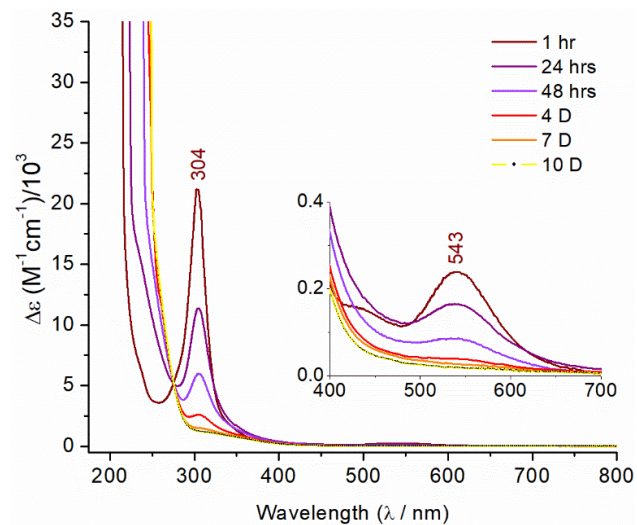
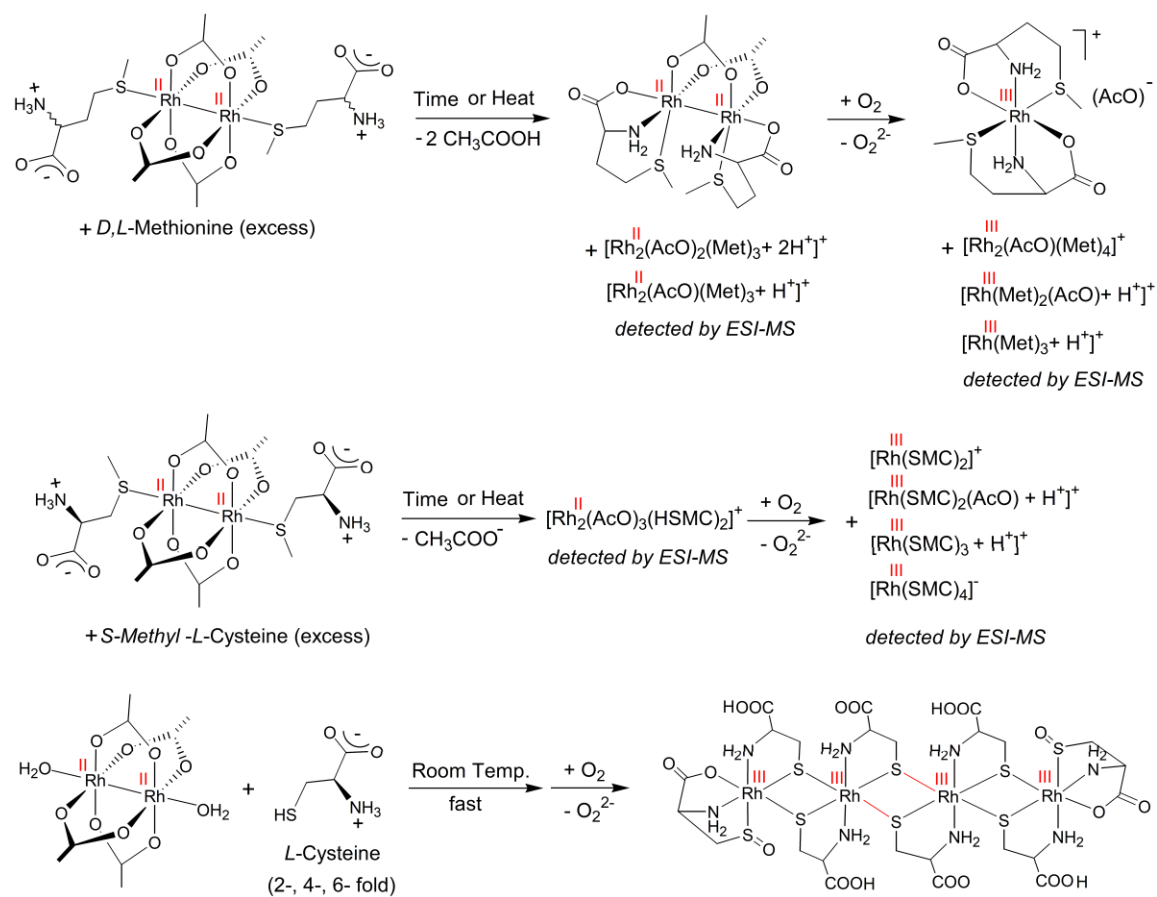


Figure 4



Scheme 2



GRAPHICAL ABSTRACT

